Journal of Quantitative Spectroscopy & Radiative Transfer 182 (2016) 219–224

Contents lists available at ScienceDirect

Journal of Quantitative Spectroscopy & Radiative Transfer

journal homepage: www.elsevier.com/locate/jqsrt

Temperature-dependent high resolution absorption cross sections of propane

Christopher A. Beale [a,*], Robert J. Hargreaves [b,c], Peter F. Bernath [b]

[a] Department of Ocean, Earth and Atmospheric Sciences, Old Dominion University, Norfolk, VA, USA
[b] Department of Chemistry and Biochemistry, Old Dominion University, Norfolk, VA, USA
[c] Atmospheric, Oceanic & Planetary Physics, University of Oxford, Clarendon Laboratory, Parks Road, Oxford OX1 3PU, UK

ARTICLE INFO

Article history:
Received 1 April 2016
Received in revised form
3 June 2016
Accepted 3 June 2016
Available online 11 June 2016

Keywords:
Absorption cross sections
Fourier transform spectroscopy
Hot hydrocarbons
Infrared spectra
Propane

ABSTRACT

High resolution (0.005 cm^{-1}) absorption cross sections have been measured for pure propane (C_3H_8). These cross sections cover the 2550–3500 cm^{-1} region at five temperatures (from 296 to 700 K) and were measured using a Fourier transform spectrometer and a quartz cell heated by a tube furnace. Calibrations were made by comparison to the integrated cross sections of propane from the Pacific Northwest National Laboratory. These are the first high resolution absorption cross sections of propane for the 3 μm region at elevated temperatures. The cross sections provided may be used to monitor propane in combustion environments and in astronomical sources such as the auroral regions of Jupiter, brown dwarfs and exoplanets.

1. Introduction

Propane (C_3H_8) is the second most abundant non-methane hydrocarbon (NMHC) in the Earth's atmosphere after ethane (C_2H_6) [1]. Propane and the other NMHCs only have a small radiative forcing effect on the Earth's atmosphere, nevertheless the chemistry of these molecules has a significant impact on the troposphere through the reaction with the hydroxyl radical (OH), which leads to the formation of acetone. This reaction also leads to the production of peroxyacetyl nitrate (PAN) [2], which has a relatively long lifetime in the upper troposphere where it acts as a reservoir for NO_x, a catalyst for the production of ozone [3].

Propane has been identified in a number of Solar System objects. These include the atmospheres of Jupiter, from observations with the Galileo Probe Neutral Mass Spectrometer [4], and Saturn, using the TEXES instrument on NASA's Infrared Telescope Facility [5]. For both planets, emission lines from the ν_{21} band (748 cm^{-1}) were detected [5,6]. Propane has also been detected on Titan, first in the stratosphere with infrared spectra from Voyager 1 [7–9] and more recently with TEXES [10] and the CIRS instrument onboard Cassini [11,12]. Efforts to accurately quantify the propane concentration on Jupiter, Saturn and Titan have suffered from a lack of reliable spectroscopic data [11,13] or laboratory spectra of sufficient resolution [5] for the regions covered by these instruments.

On board NASA's Juno mission [14] is the Jovian Infrared Auroral Mapper (JIRAM) [15], which is due to arrive at Jupiter in July 2016. The JIRAM spectrometer covers the 2–5 μm range and will be used to study hot emission in Jupiter's auroral regions that has been assigned to H_3^+ and a number of hydrocarbon species [16]. Although the JIRAM spectrometer has a relatively low spectral resolution, it has previously been shown [11] that recent high resolution propane spectra in the 7–15 μm regions [13] were crucial

* Corresponding author.
E-mail address: cbeale@odu.edu (C.A. Beale).

http://dx.doi.org/10.1016/j.jqsrt.2016.06.006
0022-4073/

to accurately modeling the propane contribution in low resolution spectra of Titan, and thus enabling the detection of propene (C_3H_6) [17].

The existence of propane and other hydrocarbons in the atmosphere of Jupiter, Saturn, Titan and other Solar System objects indicates the possibility of such molecules existing in the atmosphere of cool brown dwarfs and exoplanets. Methane (CH_4) has already been detected in exoplanet atmospheres [18,19] and a number of additional hydrocarbons, including propane, are predicted to exist in the atmospheres of such objects [20,21]. The relatively cool temperatures of brown dwarf atmospheres result in their spectra being dominated by molecular features. Models have predicted brown dwarf atmospheres may include propane, although at much lower concentrations than methane or ethane [21]. The atmospheres of hot Jupiters and brown dwarfs provide environments at elevated temperatures that could contain complex hydrocarbons such as propane. However, the laboratory data on which spectral models for these objects rely are incomplete or not recorded under the appropriate temperatures or pressures.

Propane, an asymmetric top molecule with C_{2v} symmetry [22], has been the subject of a number of spectroscopic studies. Of the 27 fundamental modes of propane detailed in Shimanouchi [23], several have been studied at high resolution, including the ν_4 (a_1, 1476 cm^{-1}), ν_{18} (b_1, 1378 cm^{-1}), ν_{19} (b_1, 1338 cm^{-1}), ν_{24} (b_2, 1472 cm^{-1}) bands [24], the ν_9 band (a_1, 369 cm^{-1}) [25], the ν_{21} band (b_1, 748 cm^{-1}) [26], the ν_{26} (b_2, 748 cm^{-1}), $2\nu_{19}$ (a_1)-ν_{19} (b_1) (1338 cm^{-1}). High resolution absorption cross sections of the 690–1550 cm^{-1} [13] and 2550–3300 cm^{-1} [2] regions have also been measured. In the 3 μm region there are 8 C–H stretching modes (ν_1 (a_1), ν_2 (a_1), ν_3 (a_1), ν_{10} (a_2), ν_{15} (b_1), ν_{16} (b_1), ν_{22} (b_2) and ν_{23} (b_2)) of which 7 modes are allowed, with only the ν_{10} mode being forbidden [23], as such the spectrum of propane is extremely congested in this region.

Several molecular databases include data for propane. HITRAN [27] contains cross sections for propane, broadened by air, from Harrison and Bernath for 195–296.4 K at high resolution (0.015 cm^{-1}) in the range 2540–3300 cm^{-1} [2]. GEISA [28] includes cross sections for 220–2000 cm^{-1}, broadened by N_2, recorded at 296 K at a resolution of 0.25 cm^{-1}, as well as 8983 transitions in the range 700–800 cm^{-1}, the CH_2 rocking mode region at a resolution of 0.08 cm^{-1}. Absorption cross sections of propane broadened by N_2 are available from the Pacific Northwest National Laboratory (PNNL), recorded in the infrared at 278, 293 and 323 K, in the range 600–6500 cm^{-1} at medium resolution (0.1 cm^{-1}) [29]. Cross sections provided by Sung et al. [13] were also recorded, broadened by N_2, at various temperatures between 145–297 K, in the range 690–1550 cm^{-1} at resolutions of 0.0033–0.0056 cm^{-1}. Absorption cross sections for propane broadened by N_2 have been measured in the 3 μm region (2500–3400 cm^{-1}) at elevated temperatures [30], although at medium resolution (0.09 cm^{-1}) and relatively low temperatures (298, 373 and 473 K).

The efficiency of fuels and engines is important for industrial applications. The combustion reactions involved can be analyzed by sophisticated models, which include a large number of temperature dependent reactions from the constituents of fuels and the products of their combustion. To this end, spectra have been recorded to monitor a number hydrocarbons in combustion reactions [31–35].

Cross sections from high resolution spectra (0.1 cm^{-1} or better) of a number of hydrocarbons have been studied in the 3 μm region at elevated temperatures, including ethane [36], propylene (C_3H_6) [31,37], methane, ethane and ethylene (C_2H_4) [38]. Klingbeil et al. [31] have also obtained spectra of a number of larger hydrocarbons (12 in total) at 1 cm^{-1} resolution up to 500 °C. However there do not exist high resolution cross section measurements of propane for the 3 μm region. Such data are required to accurately model hot environments such as auroral regions on Jupiter, exoplanets or brown dwarfs. This paper addresses the lack of high resolution cross sections of propane at high temperature.

2. Experimental

High resolution (0.005 cm^{-1}) propane spectra were recorded between 2500 and 3500 cm^{-1}, at five temperatures from 296 K to 700 K using a Bruker IFS 125 Fourier transform spectrometer. This region contains the seven active C–H stretching modes [23] and a number of combinations and overtones of the various other modes. The propane gas (Airgas, 99.99% purity) is contained in an all quartz cell (i.e., with quartz windows) which is heated to the appropriate temperature using a tube furnace.

To obtain a transmission spectrum (τ) two individual spectra are recorded for each temperature and combined as,

$$\tau = \frac{A_{ab}}{A_{ref}}, \quad (1)$$

where the C_3H_8 absorption component is given by A_{ab} and A_{ref} is the background spectrum.

The conditions for the experiment are detailed in Table 1. At higher temperatures (600 and 700 K) there is an emission component which is significant enough that it must be corrected for. As a result two additional spectra were recorded for these temperatures without the infrared source, one with propane in the sample cell and one without. These emission spectra were subtracted from A_{ab} and A_{ref} respectively. The experimental setup and procedure for obtaining the transmission spectrum are

Table 1
Experimental conditions and setup of the Bruker 125 HR.

Spectral range (cm^{-1})	2500–3500
Temperature range (K)	296–700
Resolution (cm^{-1})	0.005
Cell path length (cm)	50
Detector	InSb
Filter	Germanium
Windows	CaF_2
Beamsplitter	CaF_2
Number of scans	300

described in detail in Hargreaves et al. [39] where it was used to produce temperature dependent line lists for CH_4 and to obtain temperature dependent cross sections for C_2H_6 [36].

The C–H stretching region contains a number of water lines that were removed using the OPUS software once the transmission spectra were obtained.

3. Results

The experimental transmission spectra are converted to absorption cross sections, σ (cm^2 $molecule^{-1}$) using the equation

$$\sigma = -\xi \frac{10^4 k_B T}{Pl} \ln\tau(\nu) \quad (2)$$

where k_B is the Boltzmann constant (1.38065×10^{-23} J K^{-1}), T is the temperature (K), P is the propane pressure (Pa), l is the optical path length (m), $\tau(\nu)$ is the transmittance at each wavenumber and ξ is a correction factor which is used to normalize the experimental cross sections to PNNL [2].

PNNL cross sections are given in units of ppm^{-1} m^{-1} at 296 K, which may be converted into units of cm $molecule^{-1}$ using the conversion $k_B \times 296 \times \ln(10) \times 10^4/0.101325$. The PNNL integrated cross sections in the region 2550–3500 cm^{-1} for 278, 293 and 323 K are 4.248×10^{-17}, 4.214×10^{-17} and 4.310×10^{-17} cm $molecule^{-1}$, respectively. The mean of the three PNNL integrated cross sections is 4.257×10^{-17} cm $molecule^{-1}$ and are within 2.3% of each other [29].

The path length of the cell can be reliably determined and the temperature of the sample was measured via a thermocouple and maintained throughout the experiment. The pressure was measured outside of the observed path and fluctuated slightly during the experiment. When calibrating to PNNL integrated cross sections, the normalization factor ξ is applied to the pressure which results in an effective pressure, i.e. the sample gas pressure required to effectively reproduce our results. In addition to these uncertainties, a small leak of air in the regulator resulted in an overestimation of the cell pressure by approximately 40 Pa. This additional pressure was sufficiently small that no adverse increase in the recorded line widths was observed. This pressure error is accounted for when calibrating to the integrated cross sections of PNNL.

The normalization factors are used to establish the effective propane pressures of the sample, which are given in Table 2. The resulting calibrated cross sections for each temperature, over the range 2550–3500 cm^{-1}, are shown in Fig. 1. The effect of normalization is that the integrated cross sections for all temperatures are equal to the mean of the PNNL cross sections, 4.257×10^{-17} cm $molecule^{-1}$.

The peak cross sections for the modes at 2887 cm^{-1} (Fig. 2), 2962 cm^{-1} and 2967 cm^{-1} are stronger at lower temperatures than at high temperatures. Each temperature was recorded at high resolution (0.005 cm^{-1}) and the evolution of the sharp, individual features of the low temperature spectra can be seen to gradually decrease to form a continuum with increasing temperature (inset Fig. 1). This is primarily caused by Doppler broadening of spectral lines and increasing populations of higher rotational states and hot bands. Fig. 2 demonstrates the temperature-dependence of the propane continuum between 2860 and 2910 cm^{-1}. The prominent P, Q and R branch structure (due to the ν_3 and ν_{16} bands) is effectively reduced to a gradual slope with no defining features over the observed temperature range.

4. Discussion

The quartz cell used to contain the sample during the experiment is assumed to be at constant temperature; these temperatures are given in Table 2. However there does exist a temperature gradient towards the ends of the cell that distorts the cross sections and contributes to the measurement error. In a separate experiment the gradient was measured with a thermocouple and found to be on the order of 2% or less (i.e., the center to end temperature difference is less than 2%). The entire cell is enclosed in the furnace in order to minimize this gradient and the temperature of the cell is measured at the center using a thermocouple with feedback to the furnace in order to maintain the set temperature. Before measurement, the furnace and cell are allowed to stabilize.

The discrepancy between the recorded pressure and the effective pressure, used to calculate the calibrated integrated cross sections, was up to 40% (at room temperature, see Table 2) and is much larger than with previous measurements. This pressure error was relatively consistent in absolute terms (around 40 Pa) and came from the propane gas tank regulator. The cell path length of 50 cm is determined to within 0.5% and the elevated temperatures (those above room temperature) are accurate to within 2%. The pressures were recorded along the same gas line as the cell using a 10 Torr MKS Baratron, which is accurate to within 0.5%. In addition to the experimental errors, photometric errors, estimated to be within 2%, were observed by variations between recorded baselines. These may be due to a number of reasons such as deposition of impurities on the cell windows, variation in the intensity of the light source over recording of the spectra and changing environmental conditions over the course of measurement, such as room temperature and humidity. The PNNL propane spectra are composites of approximately 10 pressure-path length measurements, making them suitably accurate to be used for calibration. These combined errors of our recorded spectra are therefore accounted for by calibration against the averaged

Table 2
Propane integrated cross section calibration.

Temperature (K)	Sample pressure (Pa)	Effective pressure (Pa)
296	173.85	124.64
400	216.92	176.86
500	264.11	199.32
600	375.97	340.21
700	428.63	408.59

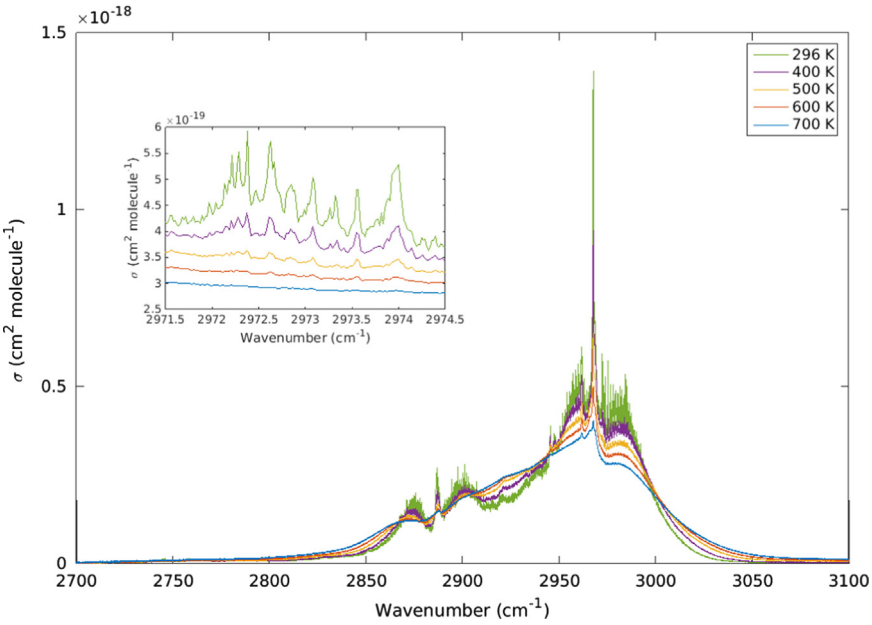

Fig. 1. Cross sections (0.005 cm^{-1} resolution) for increasing temperatures in the range 2700–3100 cm^{-1}. The inset displays a more detailed view of each spectrum (2971.5–2974.5 cm^{-1}) where the strong features are seen to weaken with increasing temperature.

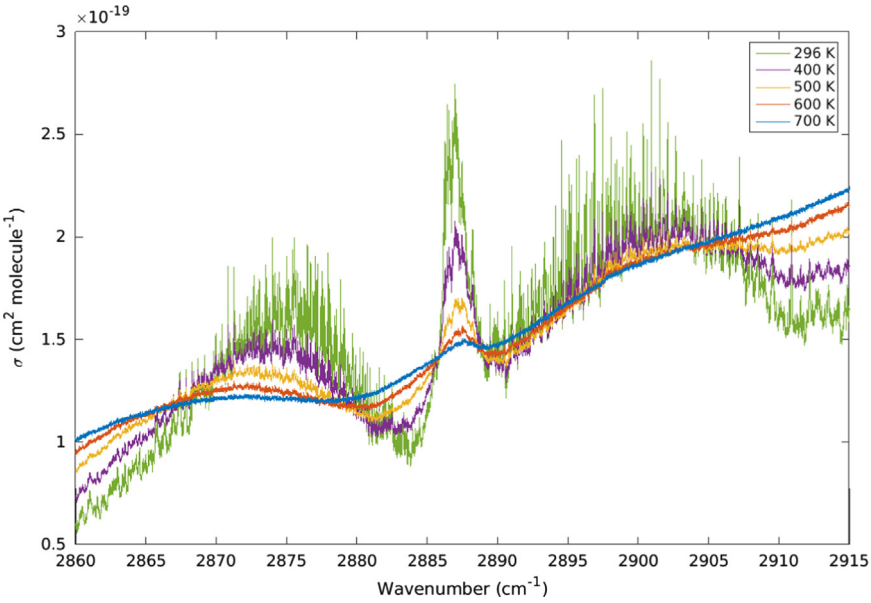

Fig. 2. A more detailed view of the ν_3 and ν_{16} modes centered at 2887 cm^{-1}. Sharp features that are identifiable in room temperature spectra blend into the continuum as the temperature increases.

integrated cross sections of the three PNNL spectra. Our estimated error in the calibrated absorption cross sections is therefore approximately 5%.

The integrated cross section over an isolated band has been shown to be independent of temperature [36,40,41]. For comparison between temperatures, the cross sections should be integrated over isolated bands, i.e. the transmission at the integration limits must be 100%. For propane, the large number of absorption bands within the observed 3 μm region (particularly at high temperature) means that complete isolation is not guaranteed. The 2550 and 3500 cm^{-1} integration limits were chosen as they provide the transmission maxima within the observed region.

The development of continua with increasing temperature has been observed in CH_4 [39] for which the large number of weak lines contribute significant absorption at higher temperatures. For larger hydrocarbons such as C_2H_6, the low frequency torsional modes result in a larger continuum effect [36]. The changing shape of the spectral features of C_3H_8 with increasing temperature in this region can be seen in Fig. 1. The populations of the low frequency

torsional modes at 216 cm^{-1} (ν_{14}, a_2) and 268 cm^{-1} (ν_{27}, b_2) increase with temperature resulting in the growth of a broad continuum.

These measurements are the first high resolution absorption cross sections of propane at high temperature and will find use in the remote sensing of propane on exoplanets, brown dwarfs and for combustion monitoring. The data is provided as supplementary material with the online version of this paper. The temperature-dependence of the propane cross section in this region makes it suitable for inferring the temperature, particularly the sharp Q branches at 2887 cm^{-1} and 2967 cm^{-1}. It is only at high resolution that many of the temperature dependent features can be identified. Certain sub-regions are also unsuitable for temperature determination of propane, for example the crossover point at 2945 cm^{-1} between the stronger continuum of the higher temperatures and the sharp features of the low temperature Q branches here shows no temperature dependence.

5. Conclusion

High resolution cross sections have been measured for pure propane in the region 2550–3500 cm^{-1} at 296, 400, 500, 600 and 700 K. The integrated cross sections were calibrated against PNNL values for the same spectral region. The calibrated cross sections cover the C–H stretching modes near 3 μm and are provided as supplementary data. These data may be included in simulations of astronomical atmospheres at appropriate temperatures, such as those of exoplanets and brown dwarfs.

Acknowledgments

Funding was provided by the NASA Planetary Atmospheres Program (Grant number: NNX14AG78G).

Appendix A. Supplementary material

Supplementary data associated with this article can be found in the online version at http://dx.doi.org/10.1016/j.jqsrt.2016.06.006.

References

[1] Doskey PV, Gaffney JS. Non-methane hydrocarbons in the Arctic atmosphere at Barrow, Alaska. Geophys Res Lett 1992;19:381–4. http://dx.doi.org/10.1029/91GL03136.
[2] Harrison JJ, Bernath PF. Infrared absorption cross sections for propane (C_3H_8) in the 3 μm region. J Quant Spectrosc Radiat Transf 2010;111:1282–8. http://dx.doi.org/10.1016/j.jqsrt.2009.11.027.
[3] Tereszchuk KA, Moore DP, Harrison JJ, Boone CD, Park M, Remedios JJ, et al. Observations of peroxyacetyl nitrate (PAN) in the upper troposphere by the Atmospheric Chemistry Experiment-Fourier Transform Spectrometer (ACE-FTS). Atmos Chem Phys 2013;13:5601–13. http://dx.doi.org/10.5194/acp-13-5601-2013.
[4] Niemann HB, Atreya SK, Carignan GR, Donahue TM, Haberman JA, Harpold DN, et al. Chemical composition measurements of the atmosphere of Jupiter with the Galileo Probe mass spectrometer. Adv Space Res 1998;21:1455–61.
[5] Greathouse TK, Lacy JH, Bézard B, Moses JI, Richter MJ, Knez C. The first detection of propane on Saturn. Icarus 2006;181:266–71, http://dx.doi.org/10.1016/j.icarus.2005.09.016.
[6] Tokunaga A, Storrs A, Beck S, Serabyn E, Bloemhof E. The detection of C_3H_8 (propane) on Jupiter. Bull Am Astron Soc 1983:832.
[7] Maguire WC, Hanel RA, Jennings DE, Kunde VG, Samuelson RE. C_3H_8 and C_3H_4 in Titan's atmosphere. Nature 1981;292:683–6.
[8] Hanel R, Conrath B, Flasar FM, Kunde V, Maguire W, Pearl J, et al. Infrared observations of the Saturnian System from Voyager 1. Science 1981;212:192–200.
[9] Kim SJ, Caldwell J. The abundance of CH_3D in the atmosphere of Titan, derived from 8 to 14 μm thermal emission. Icarus 1982;52:473–82.
[10] Roe HG, Greathouse TK, Richter MJ, Lacy JH. Propane on Titan. Astrophys J Lett 2003;597:L65. http://dx.doi.org/10.1086/379816.
[11] Nixon CA, Teanby NA, Calcutt SB, Aslam S, Jennings DE, Kunde VG, et al. Infrared limb sounding of Titan with the Cassini Composite InfraRed Spectrometer: effects of the mid-IR detector spatial responses. Appl Opt 2009;48:1912–25. http://dx.doi.org/10.1364/AO.49.005575.
[12] Coustenis A, Achterberg RK, Conrath BJ, Jennings DE, Marten A, Gautier D, et al. The composition of Titan's stratosphere from Cassini/CIRS mid-infrared spectra. Icarus 2007;189:35–62, http://dx.doi.org/10.1016/j.icarus.2006.12.022.
[13] Sung K, Toon GC, Mantz AW, Smith MAH. FT-IR measurements of cold C_3H_8 cross sections at 7–15 μm for Titan atmosphere. Icarus 2013;226:1499–513. http://dx.doi.org/10.1016/j.icarus.2013.07.028.
[14] Matousek S. The Juno new frontiers mission. Acta Astronaut 2007;61:932–9. http://dx.doi.org/10.1016/j.actaastro.2006.12.013.
[15] Adriani A, Coradini A, Filacchione G, Lunine JI, Bini A, Pasqui C, et al. JIRAM, the image spectrometer in the near infrared on board the Juno mission to Jupiter. Astrobiology 2008;8:613–22, http://dx.doi.org/10.1089/ast.2007.0167.
[16] Kim SJ, Geballe TR, Seo HJ, Kim JH. Jupiter's hydrocarbon polar brightening: Discovery of 3-micron line emission from south polar CH_4, C_2H_2, and C_2H_6. Icarus 2009;202:354–7. http://dx.doi.org/10.1016/j.icarus.2009.03.020.
[17] Nixon CA, Jennings DE, Bézard B, Vinatier S, Teanby NA, Sung K, et al. Detection of propene in Titan's stratosphere. Astrophys J Lett 2013;776:L14. http://dx.doi.org/10.1088/2041-8205/776/1/L14.
[18] Swain MR, Vasisht G, Tinetti G. The presence of methane in the atmosphere of an extrasolar planet. Nature 2008;452:329–31. http://dx.doi.org/10.1038/nature06823.
[19] Swain MR, Tinetti G, Vasisht G, Deroo P, Griffith C, Bouwman J, et al. Water, methane, and carbon dioxide present in the dayside spectrum of the Exoplanet HD 209458b. Astrophys J 2009;704:1616. http://dx.doi.org/10.1088/0004-637X/704/2/1616.
[20] Venot O, Hébrard E, Agúndez M, Decin L, Bounaceur R. New chemical scheme for studying carbon-rich exoplanet atmospheres. A&A 2015;577:A33. http://dx.doi.org/10.1051/0004-6361/201425311.
[21] Lodders K, Fegley Jr B. Atmospheric chemistry in giant planets, brown dwarfs, and low-mass dwarf stars: I. carbon, nitrogen, and oxygen. Icarus 2002;155:393–424. http://dx.doi.org/10.1006/icar.2001.6740.
[22] Lide DR. Microwave spectrum, structure, and dipole moment of propane. J Chem Phys 1960;33:1514–8. http://dx.doi.org/10.1063/1.1731434.
[23] Shimanouchi T. Tables of molecular vibrational frequencies consolidated. Washington, D.C.: National Bureau of Standards; 1972.
[24] Flaud JM, Lafferty WJ, Herman M. First high resolution analysis of the absorption spectrum of propane in the 6.7 μm to 7.5 μm spectral region. J Chem Phys 2001;114:9361–6. http://dx.doi.org/10.1080/00268970903501709.
[25] Kwabia Tchana F, Flaud JM, Lafferty WJ, Manceron L, Roy P. The first high-resolution analysis of the low-lying ν_9 band of propane. J Quant Spectrosc Radiat Transf 2010;111:1277–81. http://dx.doi.org/10.1016/j.jqsrt.2009.12.009.
[26] Perrin A, Kwabia-Tchana F, Flaud JM, Manceron L, Demaison J, Vogt N, et al. First high resolution analysis of the ν_{21} band of propane $CH_3CH_2CH_3$ at 921.382 cm^{-1}: evidence of large amplitude tunneling effects. J Mol Spectrosc 2015;315:55–62. http://dx.doi.org/10.1016/j.jms.2015.02.010.
[27] Rothman LS, Gordon IE, Babikov Y, Barbe A, Benner CD, Bernath PF, et al. The HITRAN2012 molecular spectroscopic database. J Quant Spectrosc Radiat Transf 2013;130:4–50. http://dx.doi.org/10.1016/j.jqsrt.2013.07.002.
[28] Jacquinet-Husson N, Scott NA, Chédin A, Crépeau L, Armante R, Capelle V, et al. The GEISA spectroscopic database: current and future

archive for Earth and planetary atmosphere studies. J Quant Spectrosc Radiat Transf 2008;109:1043–59. http://dx.doi.org/10.1016/j.jqsrt.2007.12.015.

[29] Sharpe SW, Johnson TJ, Sams RL, Chu PM, Rhoderick GC, Johnson PA. Gas-phase databases for quantitative infrared spectroscopy. Appl Spectrosc 2004;58:1452–61.

[30] Grosch A, Beushausen V, Wackerbarth H, Thiele O, Berg T. Temperature- and pressure-dependent midinfrared absorption cross sections of gaseous hydrocarbons. Appl Opt 2010;49:196–203, http://dx.doi.org/10.1364/AO.49.000196.

[31] Klingbeil AE, Jeffries JB, Hanson RK. Temperature-dependent mid-IR absorption spectra of gaseous hydrocarbons. J Quant Spectrosc Radiat Transf 2007;107:407–20. http://dx.doi.org/10.1016/j.jqsrt.2007.03.004.

[32] Chrystie RSM, Nasir EF, Farooq A. Propene concentration sensing for combustion gases using quantum-cascade laser absorption near 11 μm. Appl Phys B 2015;120:317–27. http://dx.doi.org/10.1007/s00340-015-6139-4.

[33] Eiji T, Nobuyuki K, Masahiro S, Atsushi N, Robert WD. In situ measurement of hydrocarbon fuel concentration near a spark plug in an engine cylinder using the 3.392 μm infrared laser absorption method: discussion of applicability with a homogeneous methane–air mixture. Meas Sci Tech 2003;14:1350.

[34] Sahlberg A-L, Zhou J, Aldén M, Li Z. Investigation of ro-vibrational spectra of small hydrocarbons at elevated temperatures using infrared degenerate four-wave mixing. J Raman Spectrosc 2016. http://dx.doi.org/10.1002/jrs.4862.

[35] Grosch A, Beushausen V, Wackerbarth H, Thiele O, Berg T, Grzeszik R. Calibration of mid-infrared transmission measurements for hydrocarbon detection and propane concentration measurements in harsh environments by using a fiber optical sensor. J Quant Spectrosc Radiat Transf 2010;112:994–1004. http://dx.doi.org/10.1016/j.jqsrt.2010.11.016.

[36] Hargreaves RJ, Buzan E, Dulick M, Bernath PF. High-resolution absorption cross sections of C_2H_6 at elevated temperatures. Mol Astrophys 2015;1:20–5. http://dx.doi.org/10.1016/j.molap.2015.09.001.

[37] Es-sebbar E-t, Alrefae M, Farooq A. Infrared cross-sections and integrated band intensities of propylene: temperature-dependent studies. J Quant Spectrosc Radiat Transf 2014;133:559–69, http://dx.doi.org/10.1016/j.jqsrt.2013.09.019.

[38] Alrefae M, Es-sebbar E-t, Farooq A. Absorption cross-section measurements of methane, ethane, ethylene and methanol at high temperatures. J Mol Spectrosc 2014;303:8–14. http://dx.doi.org/10.1016/j.jms.2014.06.007.

[39] Hargreaves RJ, Bernath PF, Bailey J, Dulick M. Empirical line lists and absorption cross sections for methane at high temperatures. Astrophys J 2015;813:12. http://dx.doi.org/10.1088/0004-637X/813/1/12.

[40] Breeze JC, Ferriso CC, Ludwig CB, Malkmus W. Temperature dependence of the total integrated intensity of vibrational–rotational band systems. J Chem Phys 1965;42:402–6. http://dx.doi.org/10.1063/1.1695707.

[41] Crawford B. Vibrational intensities. X. Integration theorems. J Chem Phys 1958;29:1042–5. http://dx.doi.org/10.1063/1.1744652.